

pubs.acs.org/JPCA Article

Absorption Spectra and the Electronic Structure of Gallic Acid in Water at Different pH: Experimental Data and Theoretical Cluster Models

Natalia V. Karimova, Man Luo, Izaac Sit, Vicki H. Grassian,* and R. Benny Gerber*



Cite This: J. Phys. Chem. A 2022, 126, 190–197



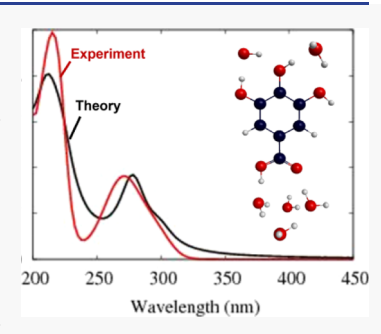
ACCESS I

Metrics & More

Article Recommendations

Supporting Information

ABSTRACT: Gallic acid (GA) has been characterized in terms of its optical properties in aqueous solutions at varying pH in experiments and in theoretical calculations by analyzing the protonated and deprotonated forms of GA. This work is part of a series of studies of the optical properties of different carboxylic acids in aqueous media. The experimental electronic spectra of GA exhibit two strong well-separated absorption peaks (B- and C-bands), which agree with previous studies. However, in the current study, an additional well-defined low-energy shoulder band (A-band) in the optical spectra of GA was identified. It is likely that the A-band occurs for other carboxylic acids in solution, but because it can overlap with the B-band, it is difficult to discern. The theoretical calculations based on density functional theory were used to simulate the optical absorption spectra of GA in water at different pH to prove the existence of this newly found shoulder band and to describe and characterize the full experimental optical spectra of



GA. Different cluster models were tested: (i) all water molecules are coordinated near the carboxy-group and (ii) additional water molecules near the hydroxy-groups of the phenyl ring were included. In this study, we found that both the polarizable continuum model (dielectric property of a medium) and neighboring water molecules (hydrogen-bonding) play significant roles in the optical spectrum. The results showed that only an extended cluster model with water molecules near carboxy- and hydroxy-groups together with the polarizable continuum model allowed us to fully reproduce the experimental data and capture all three absorption bands (A, B, and C). The oscillator strengths of the absorption bands were obtained from the experimental data and compared with theoretical results. Additionally, our work provides a detailed interpretation of the pH effects observed in the experimental absorption spectra.

1. INTRODUCTION

Gallic acid (GA)(3, 4, 5 trihydroxy benzoic acid) is a naturally occurring low-molecular-weight triphenolic compound. This molecule was found to have significant biological activity, including anti-flammatory, anti-fungal, and anti-viral activities. GA is also an important antioxidant that exhibits anticancer and anti-mutagenic activity. GA and its esters are industrially important chemicals used in the food and pharmaceutical industries. It is an important precursor for many synthetic compounds and has been used as a source material for paints, ink dyes, and in the manufacturing of paper. S

GA is a phenolic acid where the carboxy-group and three hydroxy-groups are attached to a phenyl ring. Quantum chemical calculations propose an entirely planar geometry with the three adjacent hydroxy-groups oriented in the same direction. Although a significant number of experimental and theoretical studies related to the optical properties of this molecule can be found in the literature, Although as studies state that the electronic spectrum of GA has only two strong well-separated absorption peaks, assigned to $n \to \pi^*$ and $\pi \to \pi^*$ -type transitions. Additionally, it was demonstrated that the peak positions and intensities vary with changes in the pH and the solvent. Badhani and Kakkar Although the solvent of the carbox of the car

found that a lower pH (up to 7) leads to a blue shift, which can be related to the deprotonation of the carboxy-group. Increasing the pH above 7 leads to the formation of the dianion after the deprotonation of a hydroxy-group, which can be associated with a red shift of the GA spectra. Earlier experimental studies 12,13 showed that the p $K_{\rm a2}$ of GA is around 8.6. However, theoretical models of GA considered in these papers 6,11 could not successfully reproduce the experimental low-energy bands of the optical spectrum at high pH.

Moreover, GA is a photochemically active molecule. Cossu and co-workers showed that the antibacterial effect of GA was attributed to the photo-irradiation of GA by UV-A light, and thus, GA can be used as a photosensitizer. This feature makes GA a model for more complex photochemical systems, including humic substances and marine chromophoric dissolved organic matter (*m*-CDOM) found in the sea surface microlayers and, more recently, found within sea spray

Received: August 19, 2021 Revised: December 13, 2021 Published: January 6, 2022





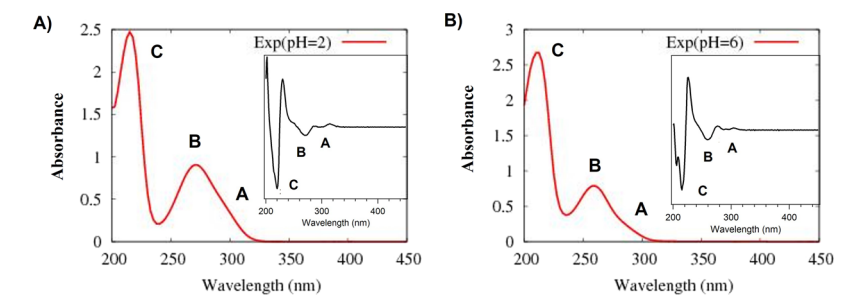


Figure 1. Experimental UV—vis spectra of 0.1 mM GA in aqueous solutions at pH 2 (A) and pH 6 (B). The inset shows the second derivative of the spectrum to better identify peaks A, B, and C that contribute to the spectrum.

Table 1. Optical Absorption Spectra: Experimental Data for GA in Water at pH 2 and 6; and Theoretical Spectral Data for an Isolated GA Molecule and Hydrated $GA \cdot (H_2O)_4$ and $GA \cdot (H_2O)_4 (H_2O)_m$ Clusters $(B3LYP/6-311++G^{**}$ Combined with C-PCM)

system	experiment at pH = 2/neutral GA model			experiment at pH = 6/ionized GA model		
band	A (nm)	B (nm)	C (nm)	A (nm)	B (nm)	C (nm)
		E	xperiment			
experiment	295	271	215	287	259	211
			Theory ^a			
GA		280	207		244	206
$GA \cdot (H_2O)_1$		281	207		249	208
$GA \cdot (H_2O)_2$		280	207		253	207
$GA \cdot (H_2O)_3$		279	207		255	207
$GA \cdot (H_2O)_4$		278	207		256	207
$GA \cdot (H_2O)_4 (H_2O)_1$	290	267	207	270	253	210
$GA \cdot (H_2O)_4 (H_2O)_2$	299	278	211	273	250	210

^aTheoretical data correspond to the maxima of the convoluted spectra obtained from the vertical excitations.

aerosols. ^{14–16} The role of *m*-CDOM as a photosensitizer, which can also play a significant role in atmospheric chemistry, is currently under investigation. Unfortunately, the structure of *m*-CDOM is complex and it contains many compounds, most of which are still not known. We are performing a series of studies of the photochemistry of individual organic compounds (such as carboxylic acids) in aqueous media through a theoretical—experimental collaboration which allows for a better understanding of the nature of m-CDOM. ^{17–20} For example, it helps with the identification of the contributing species and chromophores.

The current work is a continuation of our previous studies related to the investigation of m-CDOM. GA is a promising model system for m-CDOM and can be used to better understand the environmental effects of pH and solvation. To study the optical properties of GA in aqueous solutions at different pH, experimental spectroscopic measurements were combined with theoretical calculations to study. This study should provide theoretical insights into the optical and electronic properties of both: the non-dissociated molecule (low pH) and the anionic, deprotonated speciated form (high pH) of GA. Experimental measurements were performed for GA with a concentration of 0.1 mM in water. To distinguish between GAs, two speciated forms in experiments, the UV-vis experiments are carried out at pH = 2 and pH = 6, which correspond to the two different species: protonated and deprotonated forms, respectively, as GA has a p K_{a1} of 4.3.¹²

Calculations of the excitation energies and oscillator strength were performed using time-dependent density functional theory $(TDDFT)^{21}$ for two types of small clusters (both neutral and anionic forms): (i) $GA \cdot (H_2O)_n$ (where n = 0-4)

and (ii) $GA \cdot (H_2O)_4 (H_2O)_m$ (with m = 1, 2). To validate the TDDFT results, algebraic diagrammatic construction $(ADC)^{22-24}$ calculations were additionally performed (see the Supporting Information). Solvent effects could play an essential role in the reactions that occur in aqueous condensed phases or at aqueous surfaces^{25–28} and significantly affect the photochemical properties of solvated species. 17-20 In this work, solvent effects were included using two methodsexplicit water molecules were combined with a continuum representation for the extended solvent environment (conductor-like polarizable continuum model, C-PCM). This gives us a better understanding of the relationships between the cluster model and the continuum model. Additionally, this systematic investigation of the photoexcitation profile of GA is important for further understanding of cluster model applications for more complex organic substances such as those present in the environment.

2. EXPERIMENTAL DATA

Aqueous solutions of GA were prepared using Milli-Q water with an electric resistance of 18.2 M Ω . GA was prepared as 0.1 mM solutions. Solution pH was determined using an Oakton 700 pH meter and was adjusted by either hydrochloric acid (1 N stock solution, Fisher Chemical) or sodium hydroxide (1 N stock solution, Fisher Chemical).

UV—vis spectral information of GA obtained using a PerkinElmer Lambda 35 UV-VIS spectrometer in the wavelength range from 200 to 450 nm in water at acidic and basic pH is shown in Figure 1. For these experiments the wavelength accuracy was ± 0.1 nm, and the bandwidth was 1 nm with a scan time of 240 nm/min. Solutions of 0.1 mM GA at different

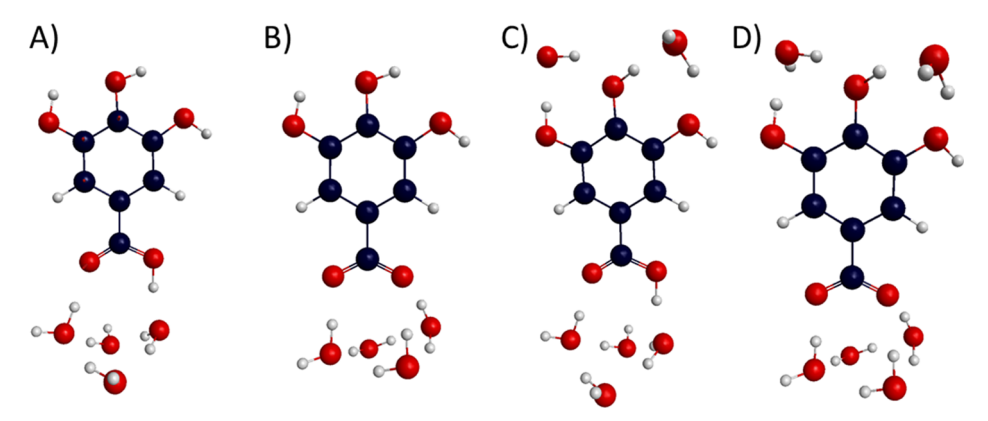


Figure 2. Structure of different cluster models: (a) neutral $GA \cdot (H_2O)_4$, (b) ionized $GA \cdot (H_2O)_4$, (c) neutral $GA \cdot (H_2O)_4$ and (d) ionized $GA \cdot (H_2O)_4$ (H₂O)₂.

pH were placed in a quartz cell with a 1 cm path length. Two strong and well-separated B- and C-bands and one shoulder A-band were found in the spectra of GA at both pH. The C-band peak maximum for the neutral and anion species were found to be centered at 215 and 211 nm, respectively. The B-band has the peak maximum centered at around 271 and 259 nm for neutral and anion species, respectively. The A-band is a broad shoulder in the spectrum. The second derivative curve (Figure 1 insert) from the UV—vis spectrum allowed us to better indicate the A-band position and the wavelength range for all these bands (A—C) (see Table 1).

3. COMPUTATIONAL METHODS

In the current work, experimental UV-vis spectra of GA were obtained in a water solution. Therefore, it is necessary to take solvent effects into account for simulations of the UV spectra. Cluster preparation was as follows. Theoretical calculations were performed for a neutral molecule of GA (low pH model) and its anion (high pH model) in the gas phase and stabilized by several water molecules. The geometries of the obtained structures were optimized using method B3LYP/6-31+G*. Different cluster models were considered: (i) $GA \cdot (H_2O)_n$ (where n = 0-4)—in this model all water molecules are coordinated by the carboxy-group of GA (Figure 2a). To get these structures, we used clusters of benzoic acid (BA) with water molecules from our previous work, 19 where we substituted three hydrogen atoms in the aromatic ring of BA with three OH groups in an orientation similar to the crystal structure of GA.²⁹ Orientations of the water molecules were retained as they were in the BA water clusters. The geometry of the obtained structures was optimized (Figure 2a,b). (ii) The second model is $GA \cdot (H_2O)_4 (H_2O)_m$ (with m = 1, 2). One and two water molecules were added to the $GA \cdot (H_2O)_4$ cluster coordinated by hydroxy-groups of the aromatic ring (Figure 2c,d). Considered conformers of the $GA \cdot (H_2O)_4 (H_2O)_m$ (with m = 1, 2), the clusters and their relative energies can be found in Figures S1 and S2. All calculations were performed using the Q-Chem program.³⁰ Geometry optimizations employ the B3LYP functional³¹ and basis set 6-31+G*. Additionally, for hydrated species, dispersion corrections from Grimme's DFT-D2 method were used.³²

Excitation spectra were calculated using the TDDFT.²¹ Our previous study for BA¹⁹ showed that the aug-cc-pVTZ and 6-311++G** basis sets provide very close results to the large aug-cc-pVQZ basis set results. Therefore, in the current study, the standard People basis set (6-311++G**) together with a

method such as B3LYP^{33,34} was chosen for the molecular orbital analysis and UV spectra calculations.^{35,36} The absorption spectra are convoluted with a Lorentzian with a full width at half-maximum of $\sigma=25$ nm.

Additionally, in our previous study, we found that solvent effects are very important for reproducing the correct optical spectra of BA species, 19 and only the combination of explicit and implicit solvent effects allowed us to reproduce the optical absorption spectrum of the deprotonated form of BA. Thus, in this study, the explicit solvent molecules (water clusters in our suggested models) were combined with the polarizable continuum model (C-PCM)³⁷ as well. The C-PCM was employed in combination with the B3LYP/6-311++G** method. Solute cavities are constructed from a union of atom-centered spheres whose radii are 1.2 times the atomic van der Waals radii suggested by Bondi.³⁸ To describe the nature of the excited states, the hole/particle natural transition orbital (NTO)^{39,40} pairs were calculated for every excited state involved in the formation of A-, B-, and C-bands for both speciated forms of GA.

High-level calculations such as the ADC²²⁻²⁴ were performed as the benchmark TDDFT. The ADC(3) and ADC(2) methods with $6-311+G^*$ and $6-311++G^{**}$ basis sets were applied for simulation of the optical absorption spectrum of the global minimum of the isolated neutral GA molecule with and without C-PCM (Supporting Information, Figure S3). We found that all three methods exhibit very similar excited states related to A-, B-, and C-bands: number of significant excited states and their intensity. However, the maxima in each of the band positions varied (Supporting Information, Figure S3). B3LYP correctly reproduces the shape and maximum position of the strong B- and C-bands (good agreement with the experiment). However, the A-band is not visible in the calculation with the TDDFT optical spectrum because the first excited state (associated with this band) is blue-shifted; this shifting reduces the gap between the A- and B-bands, which makes the A-band shoulder not visible. In the calculated spectrum, the theoretical gap is just 13 nm, whereas according to the experiment, it should be on the order of 24 nm. ADC(n) methods also cannot reproduce the gap between the A- and B-bands correctly. The calculated gaps are 29 and 44 nm with ADC(2) and ADC(3), respectively. Additionally, the full spectrum of ADC(3) is significantly blueshifted, and there is little to no agreement with the experiment in the bands' positions (Supporting Information, Figure S3). Method ADC(2) can reproduce the high energy C-band

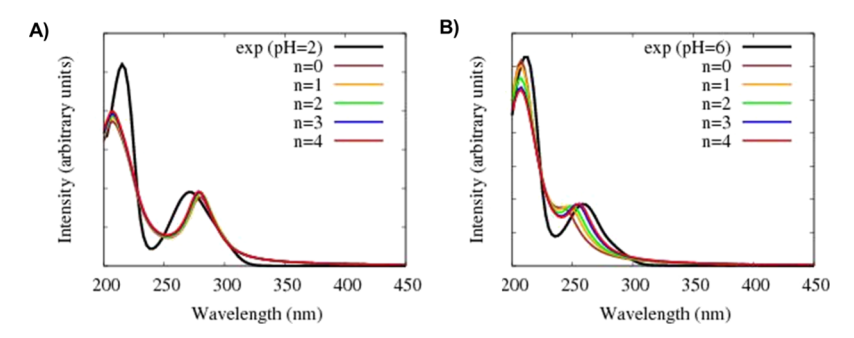


Figure 3. Experimental (black line) and theoretical (colored lines for n = 0 to 4) optical spectra of (A) neutral and (B) ionized GA water clusters— $GA \cdot (H_2O)_n$.

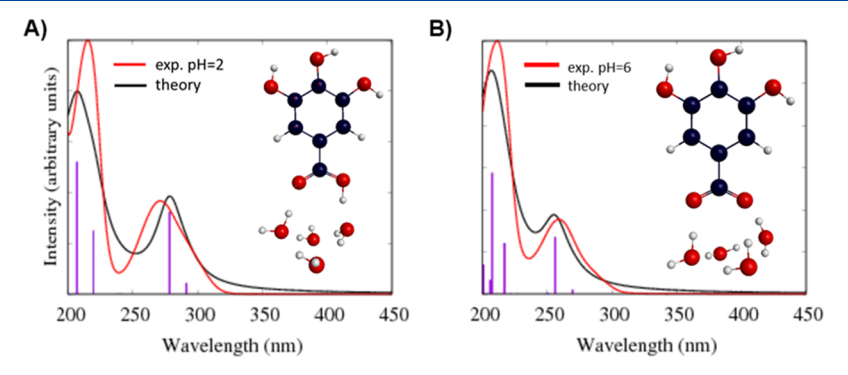


Figure 4. Experimental and theoretical optical spectra with vertical excited states of (A) neutral and (B) ionized $GA \cdot (H_2O)_4$. (B3LYP/6-311++G** with C-PCM.)

position; however, the A- and B-bands are blue-shifted by at least 25 nm. This poor performance of all theoretical methods can be related to the solvent effects of this system. To test the solvent effects on the optical spectrum calculated with B3LYP and ADC(n) methods, we added the C-PCM model to the isolated neutral GA. Unfortunately, C-PCM only is not enough, and the results for the gas phase and with C-PCM are very similar (Supporting Information, Figure S3).

Therefore, the results for the isolated GA molecule showed that TDDFT correctly reproduces the shape and maximum position of the strong B- and C-bands. Also, we found that B3LYP and ADC(n) provide very close results such as the type and intensity of the excited states. The incorrect prediction of the position of the first excited state can be related to the solvent effect, which may require combining implicit and explicit water molecules in our models. Additionally, TDDFT is computationally less expensive with respect to ADC(n) levels of theory. Therefore, in this work, we will use the B3LYP method to study the solvent and pH effects on the optical properties of GA in aqueous solutions.

4. RESULTS

4.1. Solvent Effects. Our previous studies demonstrated that solvent effects play a significant role in the optical properties of organic acids such as pyruvic acid, ¹⁷ BA, ¹⁹ and *m*-CDOM. ²⁰ For example, we obtained good agreement with the experimental spectrum of BA at high pH only when the explicit solvent molecules near the carboxy-group (water clusters in our suggested models) were combined with the polarizable continuum model. ¹⁹ A similar approach was applied in the current study.

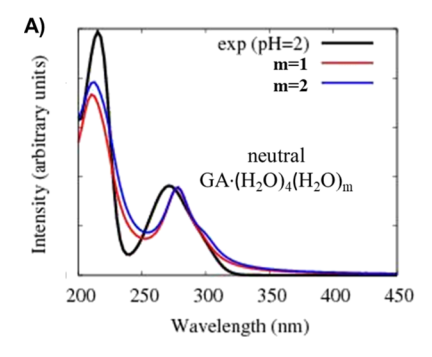
4.1.1. Model $GA \cdot (H_2O)_n$. In the first step, we consider the neutral and ionized complexes $GA \cdot (H_2O)_n$ (where n = 0-4).

In these structures, all water molecules are located by the carboxy-group (Figure 2a,b). Electronic spectra for this type of model calculated using the B3LYP method in the gas phase and with C-PCM show just two strong well-spaced B- and C-bands, with the A-band not visible on the theoretical spectra because the first excited state is blue-shifted and located closer to the B-band (Table 1, Figures 3 and 4). However, the positions of the theoretical B- and C-bands bands are in good agreement with the experiment.

Interestingly, in the case of the neutral system, the number of water molecules does not play a significant role in the position and intensity of the peaks (Figure 3a). However, the situation is changed when GA is ionized: the B-band is sensitive to hydration. Without water molecules, the B-band is poorly defined (it looks like a weak shoulder band which is significantly blue-shifted with respect to the experimental peak), see Figure 3b. However, the increased number of water molecules near the carboxy-group improved the position and intensity of the B-band. In the next step, we want to improve our model to reproduce all three experimental bands (A, B, and C). More GA—water interactions may be required to introduce all solvent effects to this molecule.

4.1.2. Model $GA \cdot (H_2O)_4(H_2O)_m$. The GA molecule, in addition to the carboxy-group, has three OH-groups. In the previous model, these three groups did not interact with explicit water molecules (all waters were located near the COOH-group). In addition to the four water molecules near the carboxy group, our new cluster model has one or two water molecules coordinated by hydroxy-groups connected to the phenyl ring (Figure 2c,d).

The results showed that two additional water molecules near hydroxy-groups improved the quality of the theoretical spectra. The new model detected all three bands, A-, B-, and C-, in the



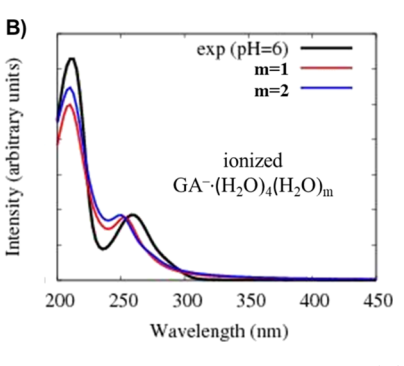
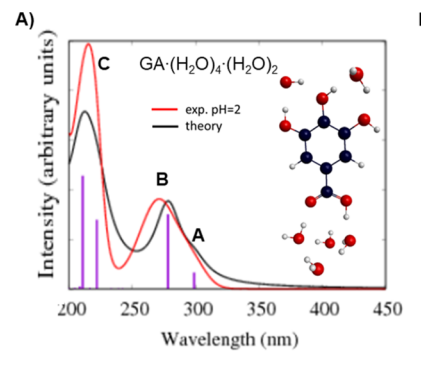


Figure 5. Experimental (black line) and theoretical (red and blue lines) optical spectra of neutral and ionized GA: (A) neutral $GA \cdot (H_2O)_4 (H_2O)_m$ and (B) ionized $GA^- \cdot (H_2O)_4 (H_2O)_m$.



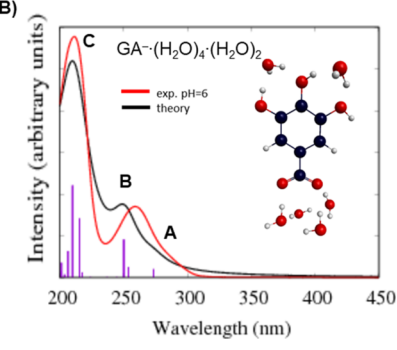


Figure 6. Theoretical optical spectra (black) and vertical excitations (purple) of neutral and ionized GA: (A) neutral $GA \cdot (H_2O)_4 (H_2O)_2$ and (B) ionized $GA^- \cdot (H_2O)_4 (H_2O)_2$.

simulated spectra of GA (Table 1, Figures 5 and 6). Excited states (responsible for the A-band formation) appeared for these new complexes: at 299 nm for the neutral system and at 273 for the ionized one. We did not have these excited states with the model $GA \cdot (H_2O)_n$ (Figure 4). Thus, the polarized continuum model cannot completely reproduce interactions between OH-groups of GA and medium water molecules. The representative model for GA in water should have the explicit water molecules near carboxy- and hydroxy-groups and should be combined with the polarizable continuum model.

Additionally, we notice that calculations of the absorption spectrum as a function of temperature were not carried out. The reason is a good agreement in the band intensities and band positions between theoretical and experimental data, which indicates that the temperature effect is not significant.

4.2. Effect of pH. Experimental results showed that the deprotonation of the carboxylic group as a result of the increase in the pH leads to a blue shift of the spectral peaks: 8, 12, and 5 nm for A-, B-, and C-bands, respectively. Both theoretically simulated absorption spectra for the neutral and ionized complexes are in good agreement with the experiment (Table 1, Figure 5). Theoretical results predicted a similar blue shift for the spectrum of the ionized $GA^-(H_2O)_4(H_2O)_2$ system when compared to neutral $GA\cdot(H_2O)_4(H_2O)_2$.

We can see that the B-band is the most sensitive to pH changes, whereas the C-band is less responsive. This may be related to the nature of orbitals involved in electron transitions formed in the excited states of these bands.

Additionally, oscillator strengths of absorption bands were obtained from the experimental data and compared with theoretical results (see Supporting Information, Table S5). Theoretical oscillator strengths are in reasonable agreement with experimental data. Theoretical oscillator strengths of low

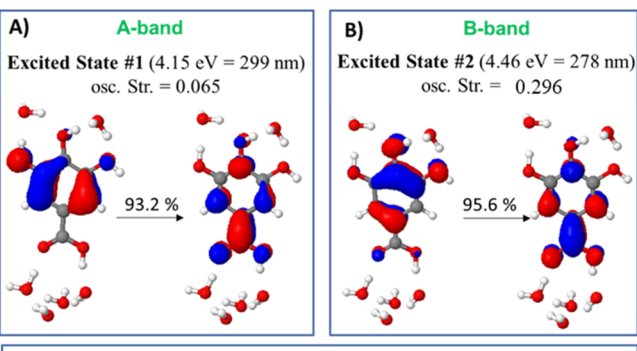
energy bands (A- and B-) are higher by about 30%, corresponding to the experiment. Experimental oscillator strengths of the C-band at both pH are significantly stronger than theoretically predicted, but it should be noticed that the theoretical C-band is a combination of several relatively strong excitations (Table S5), which makes the intensity of the theoretical C-band comparable to the experiment.

4.3. Electron Transition Analysis and Peak Characterization. To characterize the absorption peaks, the hole/particle NTO pairs were calculated for the selected excited states for both systems: neutral and ionized.

4.3.1. A-Band. The spectra show that the A-band is a shoulder peak corresponding to $\pi \to \pi^*$ type transitions for both neutral and ionized systems. The HOMO (π) orbitals are localized on the phenyl-ring and OH-groups, whereas the carboxy-group does not participate. The LUMO (π^*) orbitals are located on the entire molecule: phenyl ring and OH- and carboxy-groups (Figures 7a, 8a).

4.3.2. B-Band. We found that the nature of the B-band depends on the pH of the system. For example, in the neutral system (low pH model), the B-band arises only from $\pi \to \pi^*$ type transitions. However, in the ionized system (high pH model), the B-band corresponds to a combination of the n \to π^* and $\pi \to \pi^*$ transitions (Figure 8b). All π and π^* orbitals of both systems are delocalized over the entire molecule. However, non-bonding (n) orbitals of the ionized system are localized on the COO-fragment only, which explains the significant blue shift of the B-band with increasing pH (Figures 7b, 8b).

4.3.3. C-Band. This band arises mainly from the $\pi \to \pi^*$ transitions. This band is less sensitive to the pH changes because all participating orbitals are located on the phenyl-ring



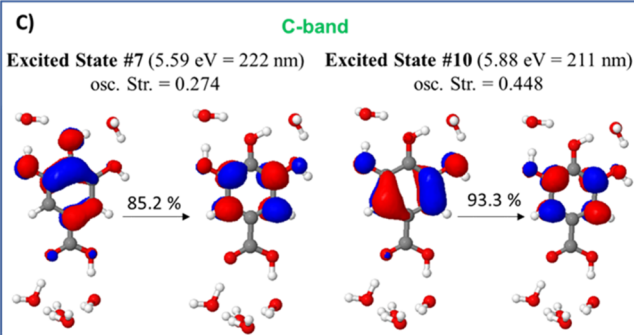


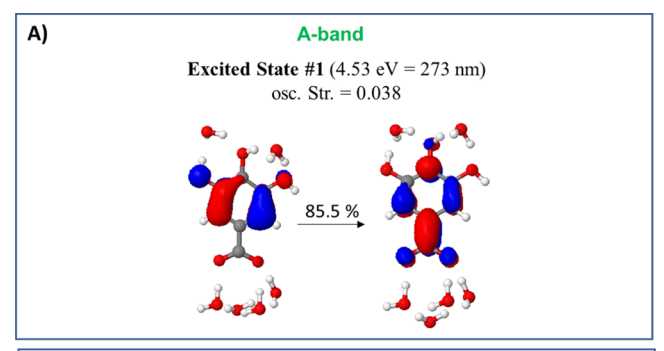
Figure 7. Orbitals of the excited states (A-, B-, and C-bands) of neutral $GA \cdot (H_2O)_4 (H_2O)_2$ calculated at the B3LYP level of theory with the basis set 6-311++G** and C-PCM. These involved electron transitions.

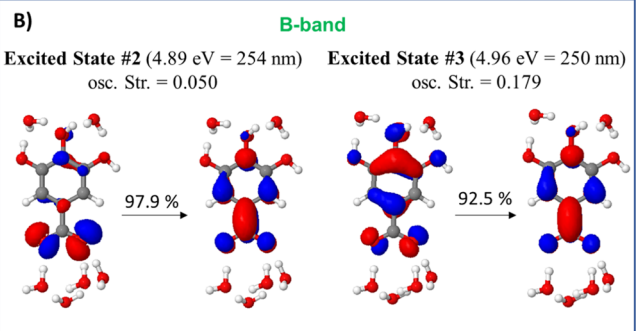
and hydroxy-groups primarily, and the orbitals of the carboxylic group are just slightly involved (Figures 7c, 8c).

5. CONCLUSIONS

In the present work, experimental spectroscopic measurements are combined with theoretical calculations to study the optical absorption spectra of GA in an aqueous solution at different pH. The current work is a continuation of our previous studies related to investigation of optical properties and the structure of the m-CDOM. It was shown that small theoretical clusters could be successful in describing chromophores and lead to correct predictions of main spectral features of organic substances in solution. Theoretical results demonstrated that solvent effects are very important for reproducing the correct optical spectra of a GA molecule at different pH. The issue of the divided role of the explicit and implicit water molecules was discussed. The representative model for GA in water should have the explicit water molecules near carboxy- and hydroxy-groups and be combined with the polarizable continuum model. Our models allowed us theoretically to reproduce all experimental bands on the optical absorption spectra of GA at different pH.

The experimental and theoretical study for the absorption spectra of GA in water found and characterized a new A-band located at 295 nm for low pH and at 287 nm for higher pH. It is likely that this band exists for other carboxylic acids in the solution but is masked by the B-band. All three absorption bands, A, B, and C, were studied and characterized experimentally and theoretically. In particular, experimental and theoretical results demonstrate that the deprotonation of the carboxylic group as a result of the increase in the pH leads to a blue shift of the spectral peaks. It was found that bands have different sensitivities to pH changes. The considered small theoretical clusters were successful in explaining this





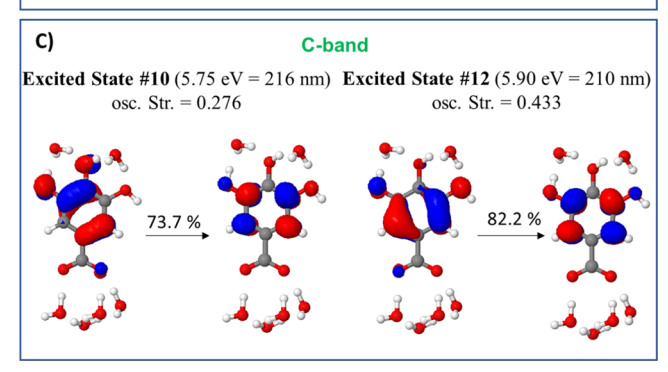


Figure 8. Orbitals of the excited states (A-, B-, and C-bands) of ionized $GA^{-}(H_2O)_4(H_2O)_2$, calculated at the B3LYP level of theory with the basis set 6-311++ G^{**} . These involved electron transitions.

phenomenon. Theoretical results showed that orbitals of the carboxy-group were actively involved in the B-band formation, especially in the case of the ionized form where the B-band arises from the mixture of the n $\rightarrow \pi^*$ and $\pi \rightarrow \pi^*$ transitions. For A- and C- bands, orbitals of the carboxy-group are slightly involved.

Overall, this is a promising model, and the theoretical approach that has been developed here can be applied to understand other molecular species in aqueous systems.

ASSOCIATED CONTENT

Supporting Information

The Supporting Information is available free of charge at https://pubs.acs.org/doi/10.1021/acs.jpca.1c07333.

Structures and their relative energies of GA· $(H_2O)_4(H_2O)_m$ and GA· $(H_2O)_4(H_2O)_m$ clusters (where m=1,2); theoretical optical spectra of the isolated neutral GA calculated using ADC(n) and B3LYP methods; theoretical optical absorption spectra for neutral GA and ionized GA clusters using the B3LYP method (in the gas phase and with C-PCM) for all considered cluster models; and excited state character-

istics such as position (eV and nm) and oscillator strength (f) for all considered cluster models (PDF)

AUTHOR INFORMATION

Corresponding Authors

Vicki H. Grassian — Department of Chemistry and Biochemistry, University of California San Diego, San Diego, California 92093, United States; o orcid.org/0000-0001-5052-0045; Email: vhgrassian@ucsd.edu

R. Benny Gerber — Department of Chemistry, University of California Irvine, Irvine, California 92697, United States; Institute of Chemistry and Fritz Haber Research Center, Hebrew University of Jerusalem, Jerusalem 91904, Israel; orcid.org/0000-0001-8468-0258; Email: robertbenny.gerber@mail.huji.ac.il

Authors

Natalia V. Karimova — Department of Chemistry, University of California Irvine, Irvine, California 92697, United States; orcid.org/0000-0002-4616-1884

Man Luo – Department of Chemistry and Biochemistry, University of California San Diego, San Diego, California 92093, United States

Izaac Sit – Department of Nanoengineering, University of California San Diego, San Diego, California 92093, United States

Complete contact information is available at: https://pubs.acs.org/10.1021/acs.jpca.1c07333

Author Contributions

N.V.K. performed theoretical simulations and wrote the first draft of the paper; M.L. made experimental measurements and calculations of the oscillator strength from the experimental optical absorption spectra; I.S. carried out calculations and curve fitting related to the experimental extinction coefficient. V.H.G. (experimental aspects) and R.B.G. (theoretical aspects) participated in the analysis of the results and conclusions and in writing/editing the paper and are corresponding authors.

Notes

The authors declare no competing financial interest. Data Availability: Additional data related to this paper can be accessed from the UC San Diego Library Digital Collections (https://library.ucsd.edu/dc/collection/bb96275693) or may be requested from the authors.

ACKNOWLEDGMENTS

The authors would like to gratefully acknowledge the support by the National Science Foundation through the Center for Aerosol Impacts on Chemistry of the Environment funded under the Centers for Chemical Innovation Program Grant CHE1801971. Additionally, this work used the Extreme Science and Engineering Discovery Environment (XSEDE),⁴¹ which is supported by grant number TG-CHE170064. The authors would also like to thank Professor Juan Navea and Dr. Dorit Shemesh for helpful discussions.

REFERENCES

- (1) Yilmaz, Y.; Toledo, R. T. Major Flavonoids in Grape Seeds and Skins: Antioxidant Capacity of Catechin, Epicatechin, and Gallic Acid. *J. Agric. Food Chem.* **2004**, *52*, 255–260.
- (2) Cháfer, A.; Fornari, T.; Stateva, R. P.; Berna, A.; García-Reverter, J. Solubility of the Natural Antioxidant Gallic Acid in Supercritical CO₂ + Ethanol as a Cosolvent. *J. Chem. Eng. Data* **2007**, *52*, 116–121.

- (3) Lu, J. J.; Wei, Y.; Yuan, Q. P. Preparative Separation of Gallic Acid from Chinese Traditional Medicine by High-Speed Counter-Current Chromatography and Followed by Preparative Liquid Chromatography. Sep. Purif. Technol. 2007, 55, 40–43.
- (4) Lu, L.-L.; Lu, X.-Y. Solubilities of Gallic Acid and Its Esters in Water. J. Chem. Eng. Data 2007, 52, 37–39.
- (5) Srivastava, V.; Saxena, H. O.; Shanker, K.; Kumar, J. K.; Luqman, S.; Gupta, M. M.; Khanuja, S. P. S.; Negi, A. S. Synthesis of Gallic Acid Based Naphthophenone Fatty Acid Amides as Cathepsin D Inhibitors. *Bioorg. Med. Chem. Lett.* **2006**, *16*, 4603–4608.
- (6) Badhani, B.; Kakkar, R. DFT Study of Structural and Electronic Properties of Gallic Acid and Its Anions in Gas Phase and in Aqueous Solution. *Struct. Chem.* **2017**, 28, 1789–1802.
- (7) Cappelli, C.; Mennucci, B.; Monti, S. Environmental Effects on the Spectroscopic Properties of Gallic Acid: A Combined Classical and Quantum Mechanical Study. *J. Phys. Chem. A* **2005**, *109*, 1933–1943
- (8) Pardeshi, S.; Dhodapkar, R.; Kumar, A. Quantum Chemical Density Functional Theory Studies on the Molecular Structure and Vibrational Spectra of Gallic Acid Imprinted Polymers. *Spectrochim. Acta, Part A* **2013**, *116*, 562–573.
- (9) Masoud, M. S.; Ali, A. E.; Haggag, S. S.; Nasr, N. M. Spectroscopic Studies on Gallic Acid and Its Azo Derivatives and Their Iron(III) Complexes. *Spectrochim. Acta, Part A* **2014**, *120*, 505–511.
- (10) Masoud, M. S.; Hagagg, S. S.; Ali, A. E.; Nasr, N. M. Solvatochromic Behavior of the Electronic Absorption Spectra of Gallic Acid and Some of Its Azo Derivatives. *Spectrochim. Acta, Part A* **2012**, *94*, 256–264.
- (11) Hostnik, G.; Tošović, J.; Štumpf, S.; Petek, A.; Bren, U. The Influence of PH on UV/Vis Spectra of Gallic and Ellagic Acid: A Combined Experimental and Computational Study. *Spectrochim. Acta, Part A* **2022**, 267, 120472.
- (12) Smith, R. M.; Martell, A. E. Critical Stability Constants; Springer: New York; London, 1989.
- (13) Ionisation Constants of Organic Acids in Aqueous Solution. In International Union of Pure and Applied Chemistry International Union of Pure and Applied Chemistry; IUPAC chemical data series; Serjeant, E. P., Dempsey, B., Eds.; Pergamon Press: Oxford; New York, 1979.
- (14) Nasser, F.; Lynch, I. Secreted Protein Eco-Corona Mediates Uptake and Impacts of Polystyrene Nanoparticles on Daphnia Magna. *J. Proteomics* **2016**, 137, 45–51.
- (15) Kwon, D.; Sovers, M. J.; Grassian, V. H.; Kleiber, P. D.; Young, M. A. Optical Properties of Humic Material Standards: Solution Phase and Aerosol Measurements. *ACS Earth Space Chem.* **2018**, *2*, 1102–1111.
- (16) Jayalath, S.; Wu, H.; Larsen, S. C.; Grassian, V. H. Surface Adsorption of Suwannee River Humic Acid on TiO $_2$ Nanoparticles: A Study of PH and Particle Size. *Langmuir* **2018**, *34*, 3136–3145.
- (17) Shemesh, D.; Luo, M.; Grassian, V. H.; Gerber, R. B. Absorption Spectra of Pyruvic Acid in Water: Insights from Calculations for Small Hydrates and Comparison to Experiment. *Phys. Chem. Chem. Phys.* **2020**, 22, 12658–12670.
- (18) Luo, M.; Shemesh, D.; Sullivan, M. N.; Alves, M. R.; Song, M.; Gerber, R. B.; Grassian, V. H. Impact of PH and NaCl and CaCl $_2$ Salts on the Speciation and Photochemistry of Pyruvic Acid in the Aqueous Phase. *J. Phys. Chem. A* **2020**, *124*, 5071–5080.
- (19) Karimova, N. V.; Luo, M.; Grassian, V. H.; Gerber, R. B. Absorption Spectra of Benzoic Acid in Water at Different PH and in the Presence of Salts: Insights from the Integration of Experimental Data and Theoretical Cluster Models. *Phys. Chem. Chem. Phys.* **2020**, 22, 5046–5056.
- (20) Karimova, N. V.; Alves, M. R.; Luo, M.; Grassian, V. H.; Gerber, R. B. Toward a microscopic model of light absorbing dissolved organic compounds in aqueous environments: theoretical and experimental study. *Phys. Chem. Chem. Phys.* **2021**, 23, 10487–10497.
- (21) Runge, E.; Gross, E. K. U. Density-Functional Theory for Time-Dependent Systems. *Phys. Rev. Lett.* **1984**, *52*, 997–1000.

- (22) Harbach, P. H. P.; Wormit, M.; Dreuw, A. The Third-Order Algebraic Diagrammatic Construction Method (ADC(3)) for the Polarization Propagator for Closed-Shell Molecules: Efficient Implementation and Benchmarking. *J. Chem. Phys.* **2014**, *141*, 064113.
- (23) Epstein, S. A.; Shemesh, D.; Tran, V. T.; Nizkorodov, S. A.; Gerber, R. B. Absorption Spectra and Photolysis of Methyl Peroxide in Liquid and Frozen Water. *J. Phys. Chem. A* **2012**, *116*, 6068–6077.
- (24) Shemesh, D.; Gerber, R. B. Molecular Dynamics of Photoinduced Reactions of Acrylic Acid: Products, Mechanisms, and Comparison with Experiment. J. Phys. Chem. Lett. 2018, 9, 527–533.
- (25) McCoy, A. B.; Garcia-Vela, A.; Gerber, R. B. Solvation Effects on Photochemical Reactions in Weakly Bound Clusters. *AIP Conference Proceedings*; AIP: Royanmont (France), 1994; Vol. 298, pp 516–527.
- (26) Vaida, V. Perspective: Water Cluster Mediated Atmospheric Chemistry. J. Chem. Phys. 2011, 135, 020901.
- (27) Neidhart, S. M.; Barngrover, B. M.; Aikens, C. M. Theoretical Examination of Solvent and R Group Dependence in Gold Thiolate Nanoparticle Synthesis. *Phys. Chem. Chem. Phys.* **2015**, *17*, 7676–7680.
- (28) Karimova, N. V.; McCaslin, L. M.; Gerber, R. B. Ion Reactions in Atmospherically-Relevant Clusters: Mechanisms, Dynamics and Spectroscopic Signatures. *Faraday Discuss.* **2019**, *217*, 342–360.
- (29) Zhao, J.; Khan, I. A.; Fronczek, F. R. Gallic Acid. Acta Crystallogr., Sect. E: Struct. Rep. Online 2011, 67, o316-o317.
- (30) Shao, Y.; Gan, Z.; Epifanovsky, E.; Gilbert, A. T. B.; Wormit, M.; Kussmann, J.; Lange, A. W.; Behn, A.; Deng, J.; Feng, X.; et al. Advances in Molecular Quantum Chemistry Contained in the Q-Chem 4 Program Package. *Mol. Phys.* **2015**, *113*, 184–215.
- (31) Becke, A. D. Density-functional thermochemistry. III. The role of exact exchange. *J. Chem. Phys.* **1993**, *98*, 5648–5652.
- (32) Grimme, S. Semiempirical GGA-Type Density Functional Constructed with a Long-Range Dispersion Correction. *J. Comput. Chem.* **2006**, 27, 1787–1799.
- (33) Eliason, T. L.; Havey, D. K.; Vaida, V. Gas Phase Infrared Spectroscopic Observation of the Organic Acid Dimers (CH₃(CH₂)₆COOH)₂, (CH₃(CH₂)₇COOH)₂, and (CH₃(CH₂)₈COOH)₂. Chem. Phys. Lett. **2005**, 402, 239–244.
- (34) Cornard, J.-P.; Lapouge, C. Absorption Spectra of Caffeic Acid, Caffeate and Their 1:1 Complex with Al(III): Density Functional Theory and Time-Dependent Density Functional Theory Investigations. *J. Phys. Chem. A* **2006**, *110*, 7159–7166.
- (35) Dunning, T. H. Gaussian Basis Sets for Use in Correlated Molecular Calculations. I. The Atoms Boron through Neon and Hydrogen. *J. Chem. Phys.* **1989**, *90*, 1007–1023.
- (36) Kendall, R. A.; Dunning, T. H.; Harrison, R. J. Electron affinities of the first-row atoms revisited. Systematic basis sets and wave functions. *J. Chem. Phys.* **1992**, *96*, 6796–6806.
- (37) Truong, T. N.; Stefanovich, E. V. A New Method for Incorporating Solvent Effect into the Classical, Ab Initio Molecular Orbital and Density Functional Theory Frameworks for Arbitrary Shape Cavity. *Chem. Phys. Lett.* **1995**, 240, 253–260.
- (38) Bondi, A. van der Waals Volumes and Radii. J. Phys. Chem. **1964**, 68, 441–451.
- (39) Plasser, F.; Thomitzni, B.; Bäppler, S. A.; Wenzel, J.; Rehn, D. R.; Wormit, M.; Dreuw, A. Statistical Analysis of Electronic Excitation Processes: Spatial Location, Compactness, Charge Transfer, and Electron-Hole Correlation. *J. Comput. Chem.* **2015**, *36*, 1609–1620.
- (40) Mewes, S. A.; Plasser, F.; Krylov, A.; Dreuw, A. Benchmarking Excited-State Calculations Using Exciton Properties. *J. Chem. Theory Comput.* **2018**, *14*, 710–725.
- (41) Towns, J.; Cockerill, T.; Dahan, M.; Foster, I.; Gaither, K.; Grimshaw, A.; Hazlewood, V.; Lathrop, S.; Lifka, D.; Peterson, G. D.; et al. XSEDE: Accelerating Scientific Discovery. *Comput. Sci. Eng.* **2014**, *16*, 62–74.

□ Recommended by ACS

Tracking Isomerizations of High-Energy Adenine Cation Radicals by UV-Vis Action Spectroscopy and Cyclic Ion Mobility Mass Spectrometry

Václav Zima, František Tureček, et al.

JULY 11, 2023

THE JOURNAL OF PHYSICAL CHEMISTRY A

READ 🖸

Guided Ion Beam Studies of the $Dy + O \rightarrow DyO^+ + e^-$ Chemiionization Reaction Thermochemistry and Dysprosium Oxide, Carbide, Sulfide, Dioxide, and Sulfoxi...

Maryam Ghiassee, P. B. Armentrout, et al.

DECEMBER 23, 2022

THE JOURNAL OF PHYSICAL CHEMISTRY A

READ 🗹

Ab Initio Calculation of Ground- and Low-Excited-State Spectroscopic Data and Transition Properties of SBr⁺

Guo-Sen Wang, Yu-Lin Wang, et al.

DECEMBER 02, 2022

THE JOURNAL OF PHYSICAL CHEMISTRY A

READ 🗹

Disentangling Multiphoton Ionization and Dissociation Channels in Molecular Oxygen Using Photoelectron-Photoion Coincidence Imaging

Ana Caballo, Daniel A. Horke, et al.

DECEMBER 21, 2022

THE JOURNAL OF PHYSICAL CHEMISTRY A

READ

Get More Suggestions >